

SnO₂/SiO₂ Nanocomposite Catalyzed One-pot, Four-component Synthesis of 2-Amino-3-Cyanopyridines

**Ajeet A. Yelwande, Madhukar E. Navgire, Deepak T. Tayde,
Balasaheb R. Arbad and Machhindra K. Lande***

Department of Chemistry, Dr. Babasaheb Ambedkar Marathwada University, Aurangabad (M.S.), 431004, India.

Received 6 December 2012, revised 14 February 2012, accepted 4 June 2012.

ABSTRACT

An efficient and rapid protocol for the synthesis of 2-amino-3-cyanopyridines by the cyclocondensation reaction of aromatic aldehydes, methyl ketones, malononitrile and ammonium acetate catalyzed by SnO₂/SiO₂ nanocomposite material at refluxed condition in ethanol was investigated. Nanocomposite (SnO₂/SiO₂) catalytic material has been synthesized by using the sol-gel method. The prepared catalytic materials were characterized by using X-ray diffraction (XRD), transmission electron microscopy (TEM), scanning electron microscopy (SEM), energy dispersive spectroscopy (EDS), Fourier transform infrared spectroscopy (FT-IR), Brunauer-Emmer-Teller (BET) surface area, and temperature-programmed desorption of ammonia (NH₃-TPD). Advantages of the present method include a simple work-up procedure, high yields of the products, low toxicity and easy recovery and reusability of the catalytic materials.

KEYWORDS

SnO₂/SiO₂, sol-gel, nanocomposite, 2-amino-3-cyanopyridines, heterogeneous catalyst.

1. Introduction

Tin oxide is an important *n*-type semiconducting material with a band gap of 3.65 ev at 300 K.¹ It has been widely used for various applications such as optoelectronic devices, fabricating solar cells, electrochemical applications, electrode material for Li-ion batteries and as gas sensors.^{2–10} Nanosized SnO₂ particles have been prepared by using chemical methods such as precipitation, hydrothermal, sol-gel, gel combustion and spray pyrolysis.^{11–18} Tin oxide and tin oxide-supported metal oxides have been extensively used as solid acid or redox catalyst for the oxidative dehydrogenation of propane, CO oxidation, esterification, reduction of NO/NO₂ to N₂ and hydrogenation of nitriles.^{19–23} For these applications, SnO₂ with small particle size or large surface area is essential to have high performance.

Recently, mesoporous SiO₂ has been proved to be significant new kind of functional material with regular channels, large surface area, high thermal stability and tunable pore sizes over a wide range. It is used in different fields such as catalysis, functional materials, nanodevices, sorption and energy storage devices.^{24–28} A composite material can be defined as a combination of two or more materials that results in better properties than those of the individual components used alone. In contrast to metallic alloys, each material retains its separate chemical, physical and mechanical properties. The main advantage of composite materials is that they provide high thermal stability and chemical resistance. The use of such a hybrid approach results in the enhancement of surface acidity (Bronsted or Lewis). Nowadays silica-supported heterogeneous materials have shown considerable importance in the field of catalysis. Hence, we report herein the catalytic application of different compositions of SnO₂/SiO₂ for the synthesis of 2-amino-3-cyanopyridines.

Many naturally occurring and synthetic compounds containing the pyridine scaffold possess interesting pharmacological

properties.²⁹ 2-Amino-3-cyanopyridines are an important class of heterocyclic compound owing to their chemotherapeutic activity such as anticancer, antitubercular, antimicrobial, anti-cardiovascular,^{30–32} etc. In addition, these compounds have also been used as ligands for the formation of transition metal complexes, in an IKK-*b*-inhibitor drug³³ and as intermediates for the synthesis of vitamins.³⁴

Numerous methods have been reported for the synthesis of 2-amino-3-cyanopyridines. This method involves the condensation of a chalcone or carbonyl compound with malononitrile and ammonium acetate. Some common procedures need multiple steps,³⁵ long reaction times, toxic benzene as solvent,³⁶ high temperature or microwave assistance,³⁷ triethylamine,³⁸ DMF,³⁹ acetic acid,⁴⁰ ethylammonium nitrate⁴¹ and [Yb(PFO)3].⁴² However, some of the commonly used methods are plagued by certain drawbacks such as long reaction time, use of volatile solvents, low yields and harsh reaction conditions. Therefore, it is necessary to develop an improved route for the synthesis of 2-amino-3-cyanopyridines under mild reaction conditions.

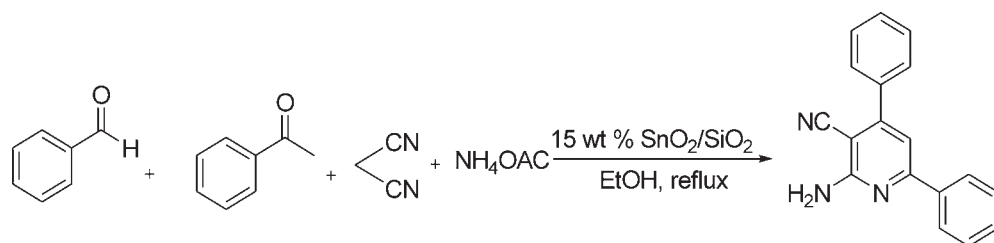
In continuation of our interest towards the development of new heterogeneous catalytic materials for the synthesis of bioactive heterocycles,^{43–45} here we report SnO₂/SiO₂ catalyzed synthesis of 2-amino-3-cyanopyridine derivatives using aromatic aldehydes, methyl ketones, malononitrile and ammonium acetate.

2. Results and Discussion

The present communication reports the one-pot four-component synthesis of 2-amino-3-cyanopyridines using SnO₂/SiO₂ as a catalyst. To optimize the reaction conditions, the reaction of benzaldehyde, acetophenone, malononitrile, and ammonium acetate was considered as a standard model reaction (Scheme 1).

This model reaction was carried out using various solvents such as methanol, acetone, acetonitrile, THF and ethanol. Results show that methanol, acetone, acetonitrile and THF

* To whom correspondence should be addressed. E-mail: mkl_chem@yahoo.com



gave moderate to good yields of 2-amino-3-cyanopyridine. However, when the reaction was run in ethanol, the yield was found relatively better (Table 1, entry 5). Therefore, ethanol was selected as a solvent for further reactions.

Similarly, in order to optimize the amount of catalyst, the model reaction was carried out in the absence and presence of various amounts of catalyst [Table 2 (a-f)]. In the absence of catalyst reaction does not proceed. Pure SiO_2 exhibits less catalytic activity in terms of reaction time and yield of the products (Table 2, entry 2b). After optimizing the model reaction it was observed that 15 wt% $\text{SnO}_2/\text{SiO}_2$ is sufficient to carry out the reaction smoothly in short time with excellent yields (Table 2, entry 2e). It was found that the use of different wt% (10%, 20%) of $\text{SnO}_2/\text{SiO}_2$ resulted in a reduction of the reaction rate and yield of the product (Table 2, entries 2d, 2f). Hence, we selected 15 wt% $\text{SnO}_2/\text{SiO}_2$ as the catalyst for the synthesis of the 2-amino-3-cyanopyridine derivatives.

Table 3 shows the generality of the present protocol for various substituted methyl ketones and a variety of aldehydes to synthesize 2-amino-3-cyanopyridines (Scheme 2). Under these conditions the yields are significantly good to excellent (82–91%). Several aromatic aldehydes bearing electron donating and electron withdrawing substituents as well as substituted methyl ketones gave good to excellent yields of the desired products.

Recyclability of a catalyst is very important from an industrial and economic point of view. Therefore, the catalyst was separated by simple filtration, washed with n-hexane and dried at 80 °C for 2 h before the next catalytic run. It was observed that such isolated catalytic material could be reused at least three times for running the conversion with similar yields under the same reaction conditions (Table 3, entry 5a).

A plausible mechanism for the synthesis of 2-amino-3-cyanopyridines is depicted in Scheme 3.⁴² The reaction may proceed via enamine 6, which is formed from reaction between the ketone and ammonium acetate, and then activated by catalyst $\text{SnO}_2/\text{SiO}_2$. From the condensation of the aldehyde with malononitrile, the alkylidene malononitrile 7 is formed. It then reacts with the enamine to give intermediate 8. In the final steps, corresponding to cycloaddition, isomerization, aromatization and aerial oxidation, the final product is obtained as shown in the scheme^{37,42}.

Table 1 Effect of various solvents on the synthesis of 2-amino-4,6-diphenylpyridine-3-carbonitrile.

Entry	Solvent	Time /h ^a	Yield /% ^b
1	Methanol	5	80
2	Acetone	6	75
3	Acetonitrile	4.5	80
4	Tetrahydrofuran (THF)	5	75
5	Ethanol	4	91

^a All reactions were carried out using $\text{SnO}_2/\text{SiO}_2$ under reflux. ^b Isolated yields.

Table 2 Effect of different weight percent of SnO_2 on the $\text{SnO}_2/\text{SiO}_2$ catalysts.

Entry	Catalyst	Time /h ^a	Yield /% ^b
2a	—	9	—
2b	SiO_2	8	35
2c	SnO_2	5.5	80
2d	10 wt% $\text{SnO}_2/\text{SiO}_2$	5	85
2e	15 wt% $\text{SnO}_2/\text{SiO}_2$	4	91 ^c
2f	20 wt% $\text{SnO}_2/\text{SiO}_2$	4.5	87

^a Reaction conditions: benzaldehyde (2 mmol), acetophenone (2 mmol), malononitrile (2 mmol), ammonium acetate (3 mmol), catalyst (0.1 g) was refluxed in 15 mL ethanol.

^b Isolated yields.

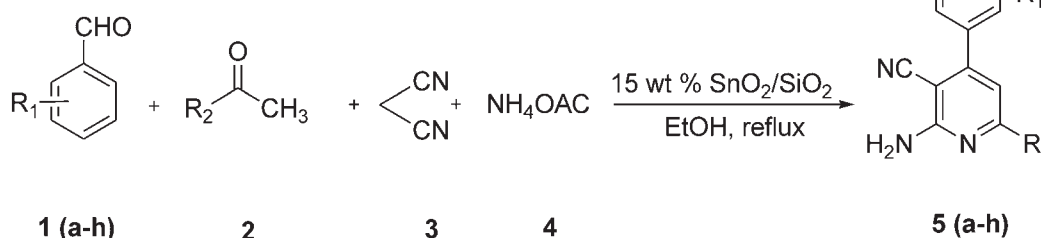
^c Reaction performed three times with average yield reported. For 2 b-d, f, yields are for single reactions.

In order to show the merits of 15 wt% $\text{SnO}_2/\text{SiO}_2$ over the reported catalysts, our results were compared with other catalysts utilized for the synthesis of 2-amino-3-cyanopyridines in Table 4. Advantages of the 15 wt% $\text{SnO}_2/\text{SiO}_2$ include a simple work-up procedure, high yields of the products, non-toxicity and easy recovery and reusability of the catalytic materials.

3. Experimental

3.1. Characterization Techniques

All chemicals were purchased from Merck and Fluka and used without further purification. Melting points were taken in an



Scheme 2.

Table 3 15 wt% SnO₂/SiO₂ catalyzed synthesis of 2-amino-3-cyanopyridine derivatives.

Entry	R ₁	R ₂	Time /h ⁻¹	Yield /% ^b	M.p. /°C
5a	H	C ₆ H ₅	4	91(91,90,90) ^c	187–189
5b	4-CH ₃	C ₆ H ₅	4.5	82	175–177
5c	4-F	C ₆ H ₅	4.5	91	217–218
5d	4-Cl	C ₆ H ₅	4	89	234–236
5e	4-Cl	4-OHC ₆ H ₄	4	87	266–268
5f	4-Cl	4-FC ₆ H ₄	4.5	82	220–222
5g	4-Cl	CH ₃	4.5	87	172–174
5h	4-Cl	4-OCH ₃ C ₆ H ₄	5	85	196–198

^a Reaction conditions: aromatic aldehydes (2 mmol), methyl ketones (2 mmol), malononitrile (2 mmol), ammonium acetate (2 mmol), catalyst (0.1 g) was refluxed in 15 mL ethanol.

^b Isolated yields.

^c Yield after consecutive cycles.

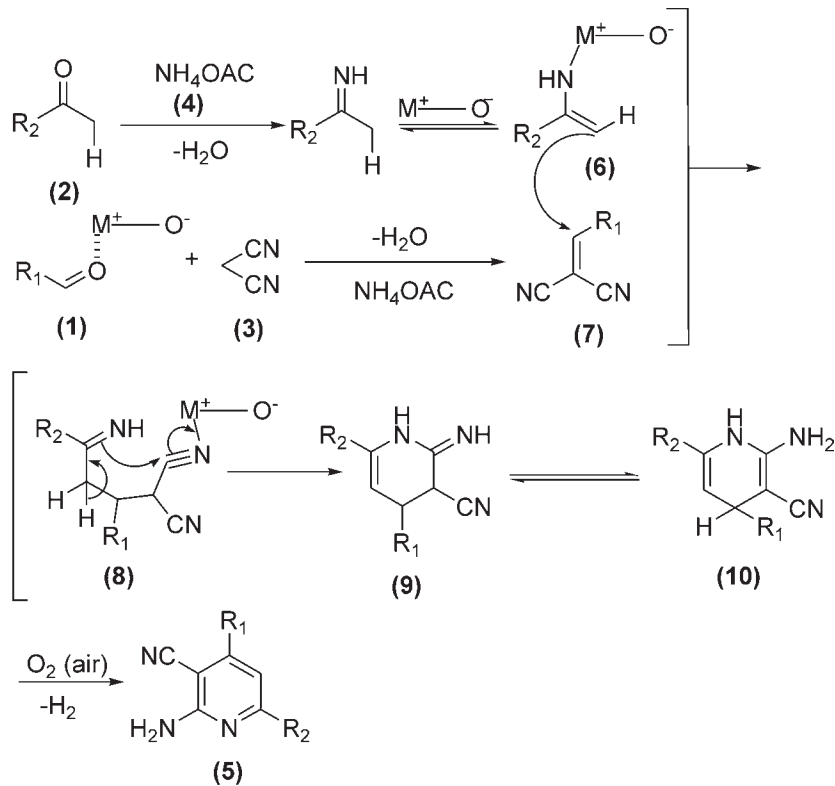
open capillary and are uncorrected. The sample morphology was characterized with CM-200 PHILIPS transmission electron microscopy (TEM) operated at 200 kv, resolution at 0.23 nm. FT-IR spectra were recorded on JASCO-FT-IR/4100, Japan, in KB disc. ¹H NMR spectra were recorded on a 300 MHz FT-NMR spectrometer in DMSO-d₆ as a solvent and chemical shift values are recorded δ (ppm) relative to tetramethylsilane (Me₄Si) as an internal standard. The X-ray diffraction (XRD) patterns were recorded on a Bruker 8D advance X-ray diffractometer using monochromator Cu-Kα radiation of wavelength = 1.5405 Å. Conventional scanning electron microscopy (SEM) images and energy dispersive spectroscopy (EDS) were obtained on JEOL; JSM-6330 LA operated at 20.0 kv and 1.0000 nA. BET surface area was measured by means of N₂ adsorption at 77.74 K preformed on a Micromeritics, ASAP 2010 and Temperature-Programmed Desorption of NH₃ (NH₃-TPD) measurements were carried out on a Micromeritics Chemisorb 2750 TPD/TPR.

3.2. Preparation of Pure Silica

Silica samples were synthesized by using a sol-gel process. Tetraethyl ortho-silicate (TEOS) (2.408 g) was placed in an autoclave bottle and 1% cetyltrimethylammonium bromide (CTAB) in 20 mL ethanol was added drop-wise with constant stirring. The pH of the reaction mixture was maintained at 10 using aqueous ammonia. This mixture was then hydrothermally treated at 60 °C for 12 h in an autoclavable bottle. After drying at 110 °C for 7 h in an oven, the obtained powder was pulverized using mortar and pestle and finally calcined at 400 °C for 2 h.

3.3. Preparation of SnO₂/SiO₂ Catalyst

A series of SnO₂/SiO₂ nanocomposite catalytic materials were synthesized by using a sol-gel method. The 15 wt% SnO₂/SiO₂ catalyst was synthesized by using 0.846 g of tin(IV) chloride dissolved in 20 mL double-distilled water and tetraethyl orthosilicate solution (2.408 g) was added drop-wise in an autoclave bottle. The resulting mixture was stirred and a 1% solution

**Scheme 3.**

Plausible mechanism for the formation of 2-amino-3-cyanopyridine.

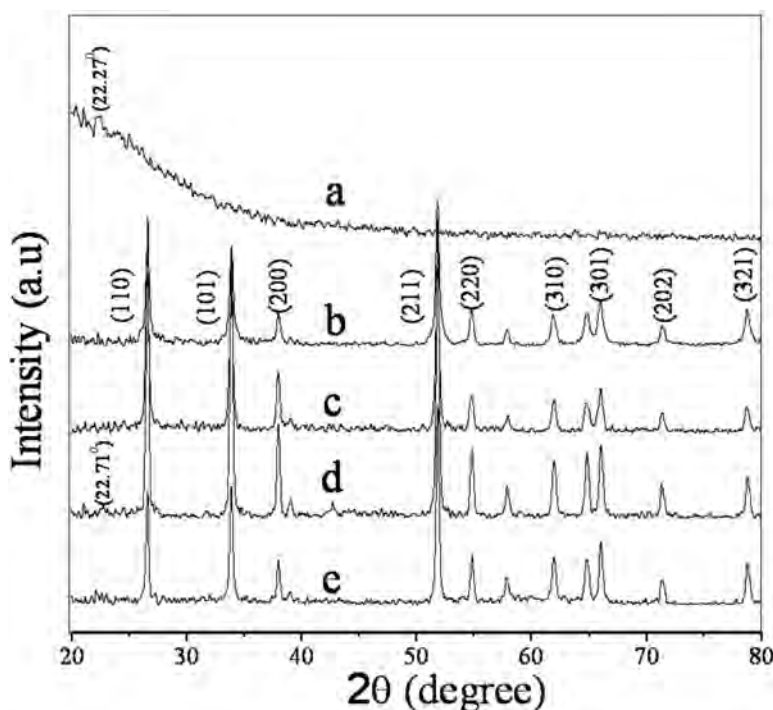


Figure 1 XRD patterns of (a) SiO_2 , (b) SnO_2 , (c) 10 wt% $\text{SnO}_2/\text{SiO}_2$, (d) 15 wt% $\text{SnO}_2/\text{SiO}_2$ and (e) 20 wt% $\text{SnO}_2/\text{SiO}_2$.

Table 4 Comparison of 15 wt% $\text{SnO}_2/\text{SiO}_2$ with other catalyst for the synthesis of 2-amino-3-cyanopyridines.

Entry	Method	Time /min	Yield /%	References
1	Microwave irradiation	7–9	72–86	37
2	ethylammonium nitrate	120–150	80–90	41
3	[Yb(PFO) ₃]	90–240	60–95	42
4	15 wt% $\text{SnO}_2/\text{SiO}_2$	240–300	82–91	a

a = this work.

of cetyltrimethylammonium bromide (CTAB) in 20 mL ethanol was added drop-wise with constant stirring. The pH of the reaction mixture was maintained at 10 using aqueous ammonia. This mixture was then hydrothermally treated at 60 °C for 12 h in an autoclavable bottle, filtered washed with distilled water then dried at 110 °C for 7 h in an oven, and the obtained powder was pulverized using mortar and pestle and finally calcined at 400 °C for 2 h. 10 wt% and 20 wt% $\text{SnO}_2/\text{SiO}_2$ catalysts were prepared in the same manner.

3.4. General Procedure for the Synthesis of 2-Amino-3-cyanopyridines (**5a–h**)

A mixture of aromatic aldehyde (2 mmol), methyl ketone (2 mmol), malononitrile (2 mmol), ammonium acetate (3 mmol) and a catalytic amount of 15 wt% $\text{SnO}_2/\text{SiO}_2$ (0.1 g) was refluxed in ethanol (15 mL) for the time as mentioned in Table 3. The progress of the reaction was monitored by thin layer chromatography in Merck pre-coated silica gel 60-F254 plates using petroleum ether: ethyl acetate as a solvent system. After completion of the reaction, the reaction mass was filtered, and the filtrate was concentrated under reduced pressure, the crude product obtained was crystallized from ethanol to afford pure products (**5a–h**)

3.4.1 Spectral Data of Representative Compound

2-amino-4,6-diphenylpyridine-3-carbonitrile (5a): IR (KBr, ν_{max}): 3363 and 3342 (NH₂), 3225 (Ar-H), 2212 (CN) cm⁻¹. ¹H NMR (300 MHz, DMSO-*d*₆) δ: 7.31–7.60 (m, 11H), 6.67 (s, 2H, NH₂).

ES-MS: *m/z* 272.15 (M⁺).

2-amino-6-phenyl-4-p-tolylpyridine-3-carbonitrile (5b): IR (KBr, ν_{max}): 3363 and 3342 (NH₂), 3225 (Ar-H), 2214 (CN) cm⁻¹. ¹H NMR (300 MHz, DMSO-*d*₆) δ: 7.08–8.04 (m, 10H), 6.85 (s, 2H, NH₂), 2.50 (s, 3H). ES-MS: *m/z* 286.10 (M⁺).

2-amino-4-(4-fluorophenyl)-6-phenylpyridine-3-carbonitrile (5c): IR (KBr, ν_{max}): 3365 and 3342 (NH₂), 3225 (Ar-H), 2212 (CN) cm⁻¹. ¹H NMR (300 MHz, DMSO-*d*₆) δ: 7.02–8.0 (m, 10H), 6.83 (s, 2H, NH₂). ES-MS: *m/z* 290.05 (M⁺).

3.5. XRD Analysis

Figure 1(a–e) shows that the XRD patterns of synthesized materials. Figure 1(a) shows the broad peak at 22.27° corresponding to the amorphous nature of silica. Figure 1(b) and (c–e) represent the XRD patterns for SnO_2 nanoparticles and $\text{SnO}_2/\text{SiO}_2$ which shows presence of highly crystalline and sharp intense peaks, which are in good agreement with that obtained by JCPDS card (411445),⁴⁶ suggesting the tetragonal lattice symmetry of this SnO_2 nano particles. Similarly, broad peaks at 22.71° in $\text{SnO}_2/\text{SiO}_2$ were observed, corresponding to the presence of amorphous silica.

3.6. TEM Image

Figure 2(a–c) shows the TEM images of synthesized materials. Figure 2(a) shows the presence of varying sphericals, which is a characteristic property of mesoporous silica having particle size in between 288–320 nm. Figure 2(b) shows the presence of flake like SnO_2 nanoparticles with an average particle size about

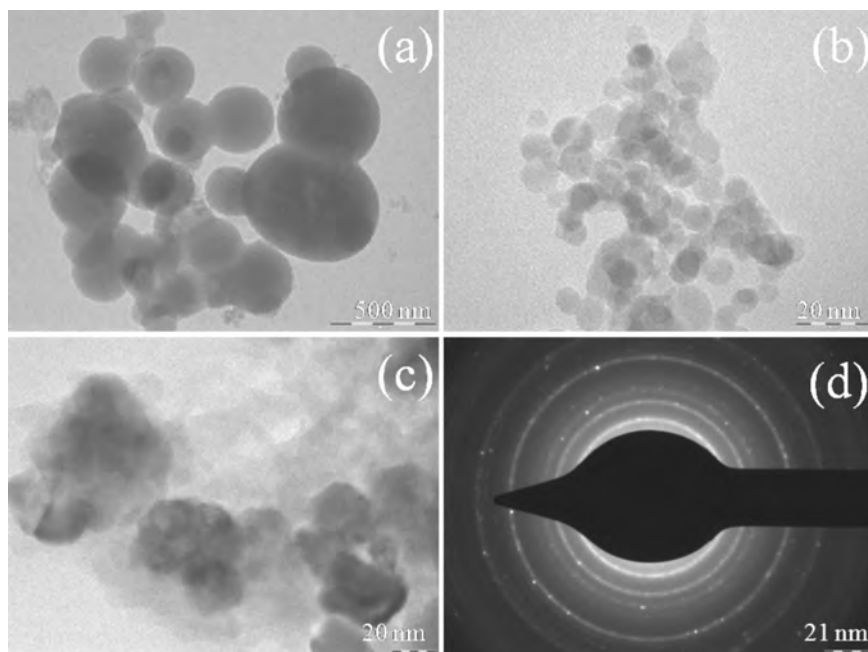


Figure 2 TEM image of (a) SiO_2 (b) SnO_2 and (c) 15 wt% $\text{SnO}_2/\text{SiO}_2$; (d) SAED patterns of SnO_2 .

7–9 nm.⁴⁷ Figure 2 (c) shows that the SnO_2 nanoparticles clearly deposited on spherical shaped SiO_2 composite and therefore, their particle size has ultimately reduced. This may be due to the reaction between Sn(OH)_4 nanoparticle and Si(OH)_4 during the polymerization process, which results in the particle size of about 25–27 nm. The selected area electron diffraction (SAED) is a crystallographic experimental technique that can be performed inside a transmission electron microscope (TEM). The typical SAED pattern for SnO_2 nanoparticle is depicted in Figure 2(d) which indicates the presence of (110), (200), (211) and (310) planes, respectively, and predict the tetragonal lattice symmetry of SnO_2 nanoparticles as evidenced from XRD analysis.

3.7. SEM-EDS Analysis

Figure 3(a–c) shows the surface morphology of synthesized

materials. Figure 3(a) shows good agglomeration of particles of mesoporous silica with a spherical shape, whereas a compact arrangement is due to uniform sized SnO_2 nanoparticles which are responsible for importing irregular shapes, Fig. 3(b).⁴⁸ Figure 3 (c–d) shows the presence of some porosity, which may be due to the insertion of 15 wt% SnO_2 nanoparticles on the surface of SiO_2 .

Energy-dispersive X-ray spectroscopy (EDS) is an analytical technique used for the elemental analysis or chemical characterization of a sample. An (EDS) spectrum of the sample with composition of 15 wt% $\text{SnO}_2/\text{SiO}_2$ catalysts gives the elemental distribution of the constituent elements and is represented in Fig. 4. The presence of constituent elements Sn, O, and Si is confirmed on the basis of atom 3.65, 54.93, and 41.44 %, respectively. This indicates that the 15 wt% $\text{SnO}_2/\text{SiO}_2$ catalyst has maintained its stoichiometric ratio.

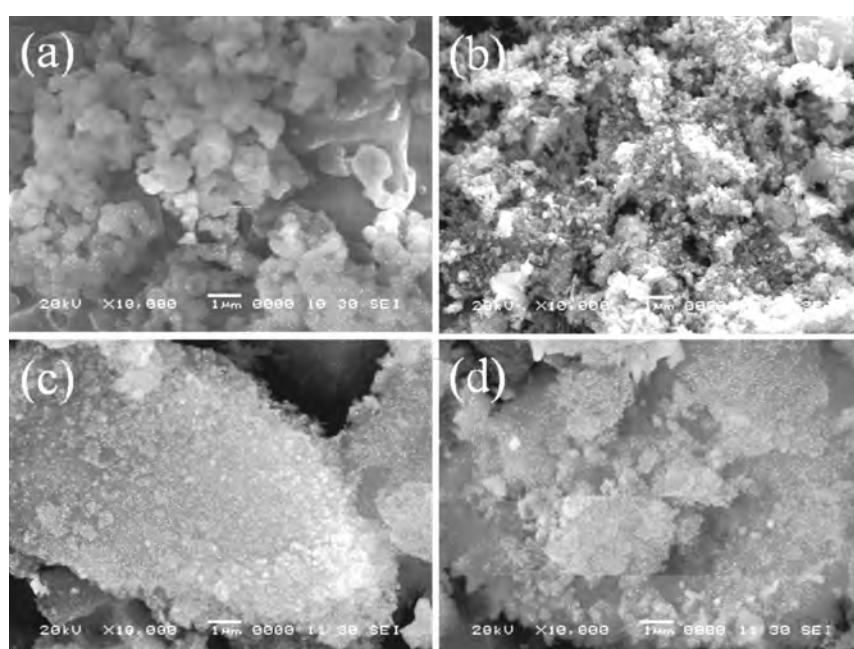


Figure 3 SEM image of (a) SiO_2 (b) SnO_2 and (c–d) 15 wt% $\text{SnO}_2/\text{SiO}_2$.

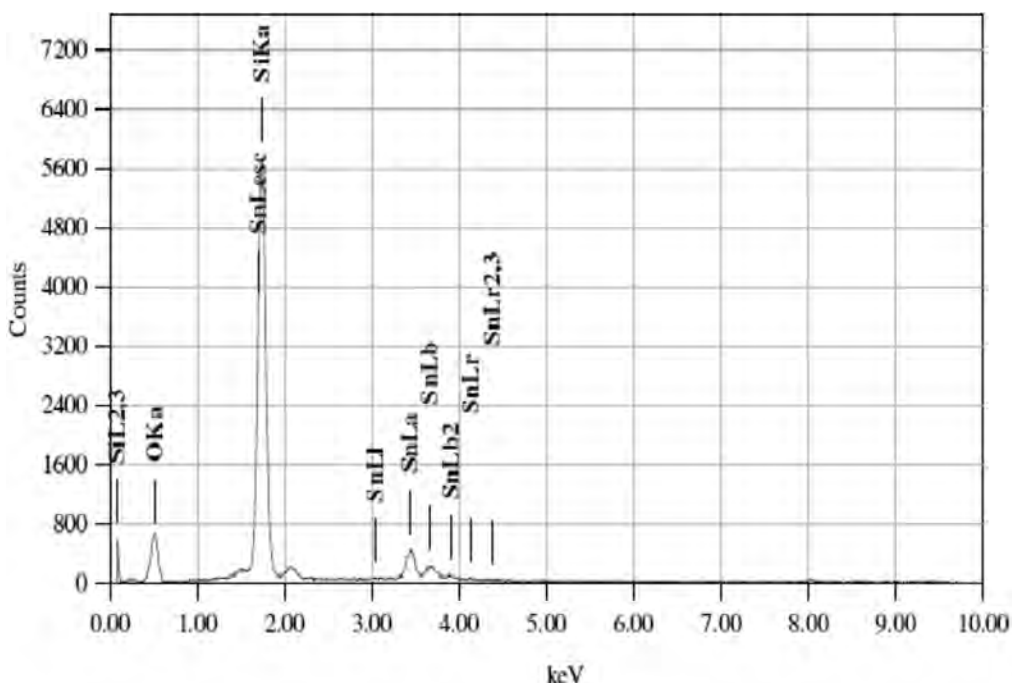


Figure 4 EDS pattern of 15 wt% $\text{SnO}_2/\text{SiO}_2$.

3.8. FTIR Analysis

Figure 5(a–e) shows the FT-IR spectra of the synthesized materials. Figure 5(a) shows the FT-IR spectrum of pure SnO_2 having absorption band at 3205 cm^{-1} which is due to the Sn-OH stretching vibration, and the band at 1634 cm^{-1} is assigned for the Sn-OH bending vibration. Figure 5(b) shows absorption band at 3410 cm^{-1} due to the Si-OH stretching vibration, 1618 cm^{-1} due to the Si-OH bending mode, 1089 cm^{-1} for Si-O stretching vibration and 806 cm^{-1} due to the Si-O-Si bending vibrational mode. The strong absorption band at 631 cm^{-1} is due to the antisymmetric Sn-O-Sn vibrational mode of SnO_2 . Similar results were reported in the literature by Deshpande *et al.*⁴⁹ Similarly, Figure 5(c–e) shows that the absorption bands at 3408 , 1620 , 1093 , 806 and 631 cm^{-1} are attributed to the $\text{SnO}_2/\text{SiO}_2$ framework.

3.9 BET and TPD Analysis

Temperature programmed desorption (NH_3 -TPD) studies were done using 100 mg of the 15 wt% $\text{SnO}_2/\text{SiO}_2$ loaded on a quartz reactor. The samples were first treated with 150°C in Helium flow 25 cc min^{-1} for 1 h at room temperature. Desorption was carried out at a heating rate of $10^\circ\text{C min}^{-1}$. Temperature programmed desorption of ammonia serves as a dependable technique for the quantitative determination of the acid strength distribution. After cooling to room temperature, ammonia was injected in the absence of the carrier gas flow and the system was allowed to attain equilibrium. A current of nitrogen was used to flush out the excess and physico-sorbed ammonia. The temperature was then raised in a stepwise manner at a linear heating rate of about $10^\circ\text{C min}^{-1}$. the ammonia desorbed from 100°C to

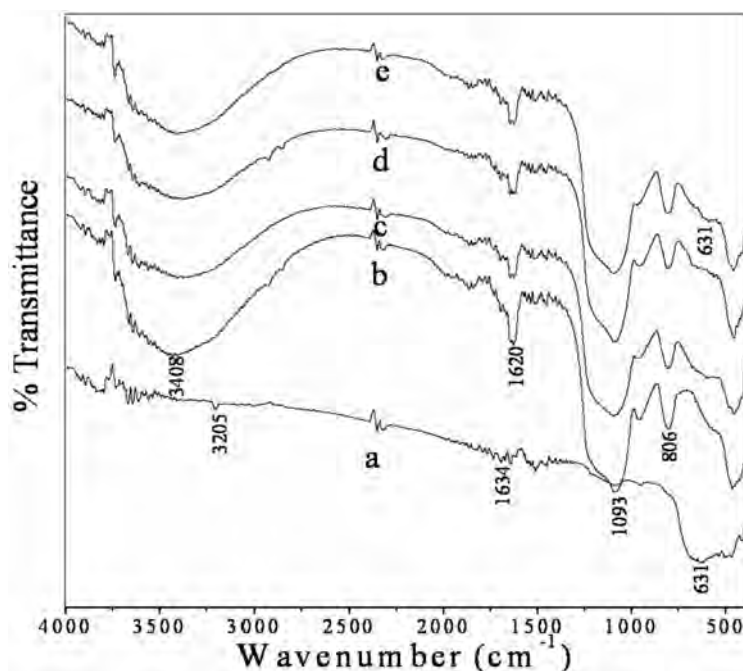


Figure 5 FT-IR patterns of (a) SnO_2 , (b) SiO_2 , (c) 10 wt% $\text{SnO}_2/\text{SiO}_2$, (d) 15 wt% $\text{SnO}_2/\text{SiO}_2$ and (e) 20 wt% $\text{SnO}_2/\text{SiO}_2$.

500 °C. Temperature Programmed Desorption method (NH_3 -TPD) was used to determine the acidic properties of solid catalyst. This provides information about the total concentration and strength of acidic sites (Bronsted and Lewis). From TPD analysis data, it was found that the ammonia desorbed in two different regions. In the first region 0.06238 mmol g⁻¹ of NH_3 desorbed at 259 °C and in the second region 0.08625 mmol g⁻¹ of NH_3 desorbed at 507.1 °C. This indicates that both the Bronsted and Lewis acidic sites are present in $\text{SnO}_2/\text{SiO}_2$ nanocomposite materials; the total acidic strength was found to be 0.149 mmol g⁻¹.

BET theory aims to explain the physical adsorption of gas molecules on a solid surface and serves as the basis for an important analysis technique for the measurement of the specific surface area of a material is the so-called BET method (Brunauer, Emmett and Teller). N_2 adsorption-desorption isotherms provide information on the textural properties of 15 wt% $\text{SnO}_2/\text{SiO}_2$ and the specific surface area. The specific surface area 331.58 m² g⁻¹ of 15 wt% $\text{SnO}_2/\text{SiO}_2$ was calculated from BET measurements.

4. Conclusion

In summary, we have synthesized series of $\text{SnO}_2/\text{SiO}_2$ catalytic materials by using sol-gel method. Synthesized catalytic materials were characterized XRD, TEM, SEM-EDS and FTIR analysis. After conformation, the catalyst was used to synthesize 2-amino-3-cyanopyridine derivatives using aromatic aldehydes, methyl ketones, malononitrile and ammonium acetate. The present method offers several advantages such as shorter reaction time, simple experimental procedure, high yield of the products and the catalyst can be recycled and reused at least three times without significant loss of activity.

Acknowledgements

The authors thank the Department of Chemistry, Dr Babasaheb Ambedkar Marathwada University, Aurangabad, India, for providing laboratory facilities, and the DST for providing financial help under the DST-FIST scheme.

References

- R. Summitt, J.A. Marley and N.F. Borrelli, *J. Phys. Chem. Solids.*, 1964, **25**, 1465–1469.
- T.W. Kim, D.U. Lee, D.C. Choo, J.H. Kim, H.J. Kim, J.H. Jeong, M. Jung, J.H. Bahang, H.L. Park, Y.S. Yoon and J.Y. Kim, *J. Phys. Chem. Solids.*, 2002, **63**, 881–885.
- T.E. Moustafid, H. Cachet, B. Tribollet and D. Festy, *Electrochim. Acta*, 2002, **47**, 1209–1215.
- M. Okuya, S. Kaneko, K. Hiroshima, I. Yagi and K. Murakami, *J. Eur. Ceram. Soc.*, 2001, **21**, 2099–2102.
- F.L. Chen and M.L. Liu, *Chem. Commun.*, 1999, **47**, 1829–1830.
- C. Kim, M. Noh, M. Choi, J. Cho and B. Park, *Chem. Mater.*, 2005, **17**, 3297–3301.
- A.J. Moulson and J.M. Herbert, *Electroceramics*, Chapman & Hall New York 1990.
- Y. Shimizu and M. Egashira, *MRS. Bull.*, 1999, **24**, 18–24.
- H.C. Wang, Y. Li and M. J. Yang, *Sens. Actuators. B. Chem.*, 2006, **119**, 380–383.
- G.J. Li, X.H. Zhang and S. Kawi, *Sens. Actuators. B. Chem.*, 1999, **60**, 64–70.
- Z.W. Chen, J.K.L. Lai and C.H. Shek, *Phys. Rev. B.*, 2004, **70**, 165314-1–165314-7.
- A. Dieguez, A. Rodriguez, R.A. Vila and J.R. Morante, *J. Appl. Phys.*, 2001, **90**, 1550–1557.
- T. Arai, *J. Phys. Soc. Jpn.*, 1960, **15**, 916–927.
- J. Jeong, S.P. Choi, C.I. Chang, D.C. Shin, J.S. Park, B.T. Lee, Y.J. Park and H.J. Song, *Solid. State. Commun.*, 2003, **127**, 595–597.
- L.R.B. Santos, T. Chartier, C. Pagnoux, J.F. Baumard, C.V. Santilli, S.H. Pulcinelli and A. Larbot, *J. Eur. Ceram. Soc.*, 2004, **24**, 3713–3721.
- B. Grzeta, E. Tkalcic, C. Goebbert, M. Takeda, M. Takahashi, K. Nomura and M. Jaksic, *J. Phys. Chem. Solids.*, 2002, **63**, 765–772.
- J.A.T. Antonio, R.G. Baez, P.J. Sebastian and A. Vazquez, *J. Solid. State. Chem.*, 2003, **174**, 241–248.
- J. Zhang and L. Gao, *J. Solid. State. Chem.*, 2004, **177**, 1425–1430.
- V.A. Sadykov, S.N. Pavlova, S.N. Saputina, I.A. Zolotarskii, N.A. Pakhomov, E.M. Moroz, V.A. Kuzmin and A.V. Kalinkin, *Catal. Today* 2000, **61**, 93–99.
- A. Hagemeyer, Z. Hogan, M. Schlichter, B. Smaka, G. Streukens, H. Turner, J.A. Volpe, H. Weinberg and K. Yaccato, *Appl. Catal. A. Gen.*, 2007, **317**, 139–148.
- A.E.R.S. Khder, *Appl. Catal. A. Gen.*, 2008, **343**, 109–116.
- J. Li, J. Hao, L. Fu, Z. Liu and X. Cui, *Catal. Today* 2004, **90**, 215–221.
- R. Gavagnin, L. Biassetto, F. Pinna and G. Strukul, *Appl. Catal. B. Env.*, 2002, **38**, 91–99.
- D.Y. Zhao, P.D. Yang, Q.S. Huo, B.F. Chmelka and G.D. Stucky, *Solid State Mater. Sci.*, 1998, **3**, 111–121.
- Y. Ren, L.P. Qian, B. Yue, and H.Y. He, *Chin. J. Catal.*, 2003, **24**, 947–950.
- S.X. Liu, B. Yue, J. Rao, Y. Zhou and H.Y. He, *Mater. Lett.*, 2006, **60**, 154–158.
- K.F. Lam, K.L. Yeung, and G. McKay, *Environ. Sci. Technol.*, 2007, **41**, 3329–3334.
- M.S. Park, G.X. Wang, Y.M. Kang, S.Y. Kim, H.K. Liu and S.X. Dou, *Electrochem. Commun.*, 2007, **9**, 71–75.
- C. Temple, G.A. Rener, W.R. Waud and P.E. Noker, *J. Med. Chem.*, 1992, **35**, 3686–3690.
- H.M. Kanjariya, T.V. Radhakrishnan, K.R. Ramchandran and P. Hansa, *Indian. J. Chem. Sect. B.*, 2004, **43**, 1569–1573.
- K.H. Popat, V.V. Kachhadia, K.S. Nimavat and H.S.J. Joshi, *Indian. Chem. Soc.*, 2004, **81**, 157–159.
- S. Jurgen, G. Siegfried, S. Alexander, B. Horst, B. Martin, G. Rainer, H. Siegbert and H. Joachim, Howard-Paul R US Patent, 1995, 5432282.
- T. Murata, M. Shimada, H. Kadono, S. Sakakibara, T. Yoshino, T. Masuda, M. Shimazaki, T. Shintani, K. Fuchikami, K.B. Bacon, K.B. Ziegelbauer and T.B. Lowinger, *Bioorg. Med. Chem. Lett.*, 2004, **14**, 4013–4017.
- J.K. Landquist, *Comprehensive Heterocyclic Chemistry*, Pergamon, Oxford, UK, 1984, 155.
- A.S. Girgis, A. Kalmouch, H.M. Hosni, *Amino Acids* 2004, **26**, 139–146.
- S. Kambe, K. Saito, *Synthesis* 1980, 366–368.
- F. Shi, S. Tu, F. Fang and T. Li, *Arkivoc* 2005, **I**, 137–142.
- E.V. Tret'yakova, O.B. Flekhter, F.Z. Galin, L.V. Spirikhin and G.A. Tolstikov, *Russ. J. Org. Chem.*, 2003, **39**, 1738–1740.
- A.M. Shestopalov and O.A. Naumov, *Russ. Chem. Bull.*, 2003, **52**, 1380–1385.
- A.N. Vasiliev, Y.S. Kayukov, O.E. Nasakin, A.N. Lyshchikov, V.N. Nesterov, O.V. Kayukova and O.V. Poulikherovskaya, *Chem. Heterocycl. Compd.*, 2001, **37**, 309–314.
- S.R. Sarda, J.D. Kale, S.K. Wasmatkar, V.S. Kadam, P.G. Ingole, W.N. Jadhav, R.P. Pawar, *Mol. Divers.*, 2009, **13**, 545–549.
- J. Tang, L. Wang, Y. Yao, L. Zhang, W. Wang, *Tetrahedron Lett.*, 2011, **52**, 509–511.
- A.A. Yelwande, B.R. Arbad and M.K. Lande, *S. Afr. J. Chem.*, 2010, **63**, 199–203.
- S.B. Rathod, M.K. Lande and B.R. Arbad, *Bull. Korean Chem. Soc.*, 2010, **31**, 2835–2840.
- A.A. Yelwande, B.R. Arbad and M.K. Lande, *J. Korean Chem. Soc.*, 2011, **55**, 644–649.
- G.J. McCarthy and J.M. Welton, *Powder. Diffr.*, 1989, **4**, 156–159.
- S. Gnanam and V. Rajendran, *Digest. J. Nanomaterials. Biostructures.*, 2010, **5**, 699–704.
- Y. Wang, C. Ma, X. Sun and H. Li, *Nanotechnol.*, 2002, **13**, 565–569.
- N.G. Deshpande, Y.G. Gudage, J.C. Ramphal Sharma Vyas, J.B. Kim and Y.P. Lee, *Sens. Actuators. B. Chem.*, 2009, **138**, 76–84.